Spin polarization through a molecular junction based on nuclear Berry curvature effects

Hung-Hsuan Teh [*]

Department of Chemistry, University of Pennsylvania, Philadelphia, Pennsylvania 19104, USA

Wenjie Dou [†]

Department of Chemistry, School of Science, Westlake University, Hangzhou, Zhejiang 310024, China;
Department of Physics, School of Science, Westlake University, Hangzhou, Zhejiang 310024, China;
and Institute of Natural Sciences, Westlake Institute for Advanced Study, Hangzhou, Zhejiang 310024, China

Joseph E. Subotnik [‡]

Department of Chemistry, University of Pennsylvania, Philadelphia, Pennsylvania 19104, USA

We explore the effects of spin-orbit coupling on nuclear wave packet motion near an out-of-equilibrium molecular junction, where nonzero Berry curvature emerges as the antisymmetric part of the electronic friction tensor. The existence of nonzero Berry curvature mandates that different nuclear wave packets (associated with different electronic spin states) experience different nuclear Berry curvatures, i.e., different pseudomagnetic fields. Furthermore, for a generic, two-orbital two-lead model (representing the simplest molecular junction), we report significant spin polarization of the *electronic* current with decaying and oscillating signatures in the large voltage limit—all as a result of *nuclear* motion. These results are consistent with magnetic AFM chiral-induced spin selectivity experiments. Altogether, our results highlight an essential role for Berry curvature in condensed phase dynamics, where spin separation survives dissipation to electron-hole pair creation and emerges as one manifestation of nuclear Berry curvature.

I. INTRODUCTION

Spintronics has a long history, originating with the famous concept of giant magnetoresistance [1]. Nowadays, there are dozens of approaches for directly manipulating spin [2–5] including: various kinds of spin injection (e.g., based on transferring photonic angular momenta to electrons), spin pumping based on transferring spin angular momenta from magnetically precessing sources to conducting spin carriers, spin-transfer torque (which is the reverse of spin pumping), and spin Seebeck effects where a thermal gradient leads to a spin current in magnetic materials. The above-mentioned concepts can be realized not only in conventional inorganic materials but also for organic molecules [6]. Most recently, there has been an enormous amount of interest in the spin Hall effect [7] (which separates different spin carriers) and the spin quantum Hall effect [8] (which allows current to flow on the surface of topological insulators without backscattering). There is no sign that progress in the arena of spintronics is slowing down.

Recently, yet another approach for manipulating spin carriers has been proposed which is based on molecular chirality—chiral-induced spin selectivity (CISS). Going back to early photoelectric experiments applied to DNA monolayers on metal surfaces [9], numerous experiments have since confirmed a CISS effect within various molecular monolayers [10], light-emitting diodes [11], and even single molecules [12]. In general, the CISS effect stipulates that, under finite voltage, the current running through a chiral set of molecules can be very spin polarized. For our purposes below, magnetic AFM CISS experiments have also been performed, whereby a monolayer of chiral molecules is in contact with a ferromagnetic material under an external magnetic field [13]; different majorities of spin sources are generated when two opposite directions of the magnetic field are applied, and correspondingly different currents are measured.

In order to explain the CISS effect, many explanations have been offered. Early on, scattering mechanisms were proposed, whereby a helical molecule can filter electrons according to angular momentum (which can be pinned to the SOC) [14]. Dephasing approaches with leakage currents (and effectively multiterminal physics) were also proposed [15]. More recently, investigations have been made not only in the linear, but also in the nonlinear response regime [16]. Overall, there is today a reasonably large list of possible CISS mechanisms (e.g., [17])—though in all cases, the necessary SOC required for large spin polarization is still too large as compared with *ab initio* calculations [18,19]. See Refs. [20,21] for a summary of recent CISS theories. At the moment, there is still no widely accepted theoretical understanding of the CISS effect.

[*]teh@sas.upenn.edu
[†]douwenjie@westlake.edu.cn
[‡]subotnik@sas.upenn.edu

Noting that nuclear motion is clearly important in DNA transport [22–24], recently we [25] and Fransson [26,27] have suggested that CISS may arise from still another source: molecular vibrations. In particular, we have pointed out that CISS may well arise from semiclassical Berry forces. Note that the influence of Berry forces is currently being explored within the quantum chemistry for small molecules with spin-orbit coupling [28], but the effect of Berry forces in the condensed phase (with friction) is not well known. The goal of this article is to explore if and how *nuclear* dynamics and Berry force may in fact lead to the manipulation of *electronic* spin in the condensed phase.

In Sec. II we demonstrate how and why a pseudomagnetic field enters the nuclear equation of motion under a Born-Oppenheimer framework. In particular, in the context of quantum transport across a molecular junction, we show that the friction tensor (which incorporates all nonadiabatic effects induced by a molecule interacting with an electronic metal bath) contains an antisymmetric component associated with the nuclear Berry curvature. These results are quite general. Thereafter, as an application, we focus on a minimal junction model with two spatial-orbital, two-nuclear, and two-spin degrees of freedom (DOF) coupled to two leads, and for such a system, we calculate the friction tensors, the covariance matrix, the adiabatic force, and the current. In Sec. III, using the quantities just described, we run dynamics and present our results for the spin current and spin polarization. We investigate a few different parameter regimes and find varying amount of spin separation; where possible, we give a phase-space microscopic explanation for the large spin polarization that we observe. Finally, in Sec. IV we conclude.

II. THEORY

A. Electronic friction, Berry curvature, and Langevin dynamics

To explain our approach, consider the standard Born-Oppenheimer ansatz [29]: a nuclear wave packet moves along on a surface corresponding to a certain electronic state I. The nuclear Hamiltonian is $\mathbf{H} = (\mathbf{P} - \mathbf{A}^I)^2/2M + \boldsymbol{\lambda}^I$, where $\mathbf{P}$ is the nuclear momentum, $\mathbf{A}^I \equiv i\hbar\langle I|\nabla|I\rangle$ is the nuclear Berry connection, and $\boldsymbol{\lambda}^I$ is the adiabatic surface of the state $|I\rangle$. The corresponding nuclear Berry curvature $\Omega_{ij} = \partial_i A_j^I - \partial_j A_i^I$ provides a pseudomagnetic field in the nuclear ij space. Notice that when a complex-valued Hamiltonian is considered (e.g., when there is electronic spin), $\mathbf{A}^I$ does not vanish and the effect of Ω_{ij} must be included for accurate dynamics on surface I [30].

Now, the discussion above was effectively predicated on modeling a small, isolated system with nuclear and electronic degrees of freedom. Within the condensed matter community, the key question is whether such effects can be meaningful in the presence of dissipative channels. To that end, in order to treat a molecule on a metal surface (where there is a continuum of electronic bath states and the system is effectively open electronically), one promising semiclassical approach is to apply an electronic friction tensor $\gamma_{\mu\nu}$ and random force ζ_μ in addition to the adiabatic force F_μ where μ and ν label nuclear space directions [31–35]. According to such a treatment, which is valid both in and out of equilibrium [31,36], provided

that the electronic bath in the metal responds quickly and a Markovian ansatz is appropriate [37], a (molecular) nuclear degree of freedom near a metal surface is driven by a Langevin equation

$$M\ddot{R}_\mu = F_\mu - \sum_\nu \gamma_{\mu\nu}\dot{R}_\nu + \zeta_\mu. \tag{1}$$

Here M is the mass of nuclei and R_μ is the nuclear position in the μ direction. Equation (1) describes dynamics on a mean-field surface such that nonadiabatic effects are included.

Consider a noninteracting Hamiltonian

$$\hat{H} = \sum_{pq} \mathcal{H}_{pq}(\mathbf{R})\hat{d}_p^\dagger \hat{d}_q + U(\mathbf{R}),$$

where $\hat{d}_p^\dagger$ ($\hat{d}_p$) creates (annihilates) an electron in orbital p and $U(\mathbf{R})$ is a purely nuclear potential energy. The friction tensor $\gamma_{\mu\nu}$, the symmetrized covariance matrix $(\bar{D}_{\mu\nu}^S + \bar{D}_{\nu\mu}^S)/2$ of the random force $\langle \zeta_\mu \zeta_\nu \rangle$ (note that only a symmetrized covariance matrix is required for running dynamics), and the adiabatic force F_μ are

$$\gamma_{\mu\nu} = \frac{\hbar}{2\pi}\int_{-\infty}^\infty d\epsilon \, \text{Tr}\{\partial_\mu \mathcal{H} \partial_\epsilon \mathcal{G}^R \partial_\nu \mathcal{H} \mathcal{G}^<\} + \text{H.c.}, \tag{2}$$

$$\frac{1}{2}(\bar{D}_{\mu\nu}^S + \bar{D}_{\nu\mu}^S) = \frac{\hbar}{8\pi}\int_{-\infty}^\infty d\epsilon \{\text{Tr}\{\partial_\mu \mathcal{H} \mathcal{G}^R(\epsilon)\partial_\nu \mathcal{H} \mathcal{G}^<(\epsilon)\}$$
$$+ \text{Tr}\{\partial_\nu \mathcal{H} \mathcal{G}^R(\epsilon)\partial_\mu \mathcal{H} \mathcal{G}^<(\epsilon)\}$$
$$+ \text{Tr}\{\partial_\mu \mathcal{H} \mathcal{G}^<(\epsilon)\partial_\nu \mathcal{H} \mathcal{G}^<(\epsilon)\}\} + \text{H.c.}, \tag{3}$$

$$F_\mu = -\frac{1}{2\pi i}\int_{-\infty}^\infty d\epsilon \, \text{Tr}\{\partial_\mu \mathcal{H} \mathcal{G}^<\} - \partial_\mu U, \tag{4}$$

where $\mathcal{G}^R$ and $\mathcal{G}^<$ are retarded and lesser Green's functions of the electron. See Appendix A for details, e.g., the derivation of Eq. (3); thereafter, the random force can be sampled by Cholesky decomposition of $(\bar{D}_{\mu\nu}^S + \bar{D}_{\nu\mu}^S)/2$. (In Appendix B we prove that the symmetrized covariance matrix is always positive definite—for a real-valued or complex-valued Hamiltonian, and for a system in or out of equilibrium.)

When contemplating Eq. (1), note that, at equilibrium, because of the fluctuation-dissipation theorem that relates $\gamma_{\mu\nu}$ to the covariance, one can use F_μ alone to determine the equilibrium density distribution (i.e. neither $\gamma_{\mu\nu}$ nor $\langle \zeta_{mu}\zeta_{nu}\rangle$ is needed); see Appendix C for a proof. Out of equilibrium, however, there is no such fluctuation-dissipation theorem and there is indeed the possibility that the steady state distribution (and therefore steady state observables, e.g., the electronic current) *will* depend on $\gamma_{\mu\nu}$ and $\langle \zeta_\mu \zeta_\nu \rangle$ as well as F_μ.

At this point, let us address $\gamma_{\mu\nu}$. The friction tensor $\gamma_{\mu\nu}$ in Eq. (1) can be divided into a symmetric part $\gamma_{\mu\nu}^S$ (which controls dissipative processes) and an antisymmetric part (which generates a Lorentz-like motion in the nuclear space and is effectively a generalization of the Berry curvature Ω_{ij}). The relative magnitudes of the symmetric and antisymmetric components can be calculated rigorously for a many-body Hamiltonian [34]. At equilibrium, previous work [30] has shown that the Lorentz-like force $\gamma_{\mu\nu}^A$ can be as large as $\gamma_{\mu\nu}^S$ (and sometimes even larger at low temperatures). In this article we will show that such a nuclear Lorentz-like force can actually lead to different electronic currents for different

spin carriers in the presence of a nonequilibrium current and voltage for a model that roughly captures the diphenylmethane molecule in a junction.

B. A generic Hamiltonian with two spatial orbitals

Consider a simple model with two spatial orbitals (1 and 2) coupled to two leads, such that the Hamiltonian depends on two nuclear degrees of freedom (x and y are considered). The total Hamiltonian $\hat{H}$ can be divided into four parts, the kinetic energy of nuclei, the subsystem (molecule) $\hat{H}_s$, the bath continuum (two leads) $\hat{H}_b$, and the subsystem-bath coupling $\hat{H}_c$,

$$\hat{H} = \frac{P^2}{2M} + \hat{H}_s + \hat{H}_b + \hat{H}_c, \tag{5}$$

$$\hat{H}_s = \sum_{pq} h^s_{pq}(\mathbf{R})\hat{b}^\dagger_p \hat{b}_q + U(\mathbf{R}), \tag{6}$$

$$\hat{H}_b = \sum_{k,\alpha=\{L,R\}} \epsilon_{k\alpha}\hat{c}^\dagger_{k\alpha}\hat{c}_{k\alpha}, \tag{7}$$

$$\hat{H}_c = \sum_{p,k\alpha} V_{p,k\alpha}\hat{b}^\dagger_p \hat{c}_{k\alpha} + \text{H.c.}, \tag{8}$$

where $\hat{b}^\dagger_p$ ($\hat{b}_p$) creates (annihilates) an electron in the subsystem spin orbital p (which is an element of $\{1,2\} \otimes \{\uparrow,\downarrow\}$), $U(\mathbf{R})$ represents a nuclear-nuclear electrostatic potential (which does not depend on any electronic degree of freedom), $c^\dagger_{k\alpha}$ ($c_{k\alpha}$) creates (annihilates) an electron in the kth spin orbital of the lead α (L/R denotes left/right lead) with the orbital energy $\epsilon_{k\alpha}$, and $V_{p,k\alpha}$ is the tunneling element between the subsystem spin orbital p and the lead spin orbital $k\alpha$. In Eq. (8), the Condon approximation has been applied (so that $V_{p,k\alpha}$ does not depend on $\mathbf{R}$); typically speaking, one can roughly recover the size of the friction tensor without incorporating non-Condon effects [38].

We focus on a shifted parabola model as a rough model for a diphenylmethane molecule in a junction:

$$\mathbf{h}^{s\uparrow} = \begin{pmatrix} x + \Delta & Ax - iBy \\ Ax + iBy & -x - \Delta \end{pmatrix}, \tag{9}$$

$$U(\mathbf{R}) = \frac{1}{2}x^2 + \kappa_x x + \frac{1}{2}\chi y^2 + \kappa_y y. \tag{10}$$

Note that such a shifted parabola model is commonly used in simulating electron transfer as well as excitation energy transfer processes [39], where the initial (single particle) state is localized on one orbital with one nuclear distribution (geometry), and the final state localizes on the other orbital with another nuclear distribution. Here Δ tunes the energy gap between two orbitals A and B control the rates at which the diabatic and spin-orbit couplings change (respectively) as a function of geometries x and y. We include a scalar potential $U(\mathbf{R})$ that tilts the overall energy landscape; such a tilt has been shown to be crucial when understanding the dynamics of photoexcited molecules relaxing through conical intersections [40]. Note that this potential does not affect the electronic friction in any way. The linear terms $\kappa_x x$ and $\kappa_y y$ effectively decrease the symmetry of the total adiabatic state and χ is the ratio of the mode-y frequency to the mode-x frequency. In practice, the scalar terms have nothing to do with spin, but as discussed below, these terms can be crucial

for generating a strong spin current. For a discussion of parameters, see Appendix D.

C. Separation of spin DOF

In principle, all orbitals in Eqs. (5)–(8) (p, q, k) are spin orbitals. However, for a system with exactly two spatial orbitals, a key observation is that, at any fixed geometry, one can always define a new spin "up" basis $|\uparrow'\rangle$ which is not coupled to the new spin "down" basis $|\downarrow'\rangle$. In other words, we can postulate that there are *two* independent Langevin equations driven by two friction tensors and random forces. This conclusion can be reached as follows (also see Appendix E for details): A general spin-orbit interaction is $\xi\mathbf{L}\cdot\mathbf{S}$ where ξ is the coupling strength, $\mathbf{L}$ is the angular momentum operator, and $\mathbf{S} = \hbar\boldsymbol{\sigma}/2$ is the spin operator. Since $\mathbf{L}_{pp}$ vanishes in all spatial directions ($p = 1, 2$), the new spin basis can be obtained by diagonalizing $\xi\mathbf{L}_{12}\cdot\mathbf{S}$ which leads to eigenvalues $\pm a$ where $a = i\hbar\xi|\mathbf{L}_{12}|/2$ is purely imaginary (note that $\mathbf{L}_{12}$ is purely imaginary). Thus, the subsystem Hamiltonian (at one geometry) becomes

$$\mathbf{h}^s = \begin{pmatrix} E_1 & W & & \\ W & E_2 & & \\ & & E_1 & W \\ & & W & E_2 \end{pmatrix}$$
$$+ \begin{pmatrix} 0 & a & & \\ a^* & 0 & & \\ & & 0 & -a \\ & & -a^* & 0 \end{pmatrix} \begin{matrix} |1\uparrow'\rangle \\ |2\uparrow'\rangle \\ |1\downarrow'\rangle \\ |2\downarrow'\rangle \end{matrix}, \tag{11}$$

where $E_{1,2}$ represent orbital energies and W denotes the diabatic coupling between the two orbitals. For all of the discussion below, we will work in this new basis, and for notational simplicity we will discard the prime. Notice that the two 2×2 blocks, defined as $\mathbf{h}^{s\uparrow}$ and $\mathbf{h}^{s\downarrow}$, are complex conjugates of each other, and the pure spin rotation that diagonalizes the term $\xi\mathbf{L}_{12}\cdot\mathbf{S}$ does not affect the orbital energies and couplings. According to Eq. (11), if we assume that the spin basis does not change (or changes weakly as a function of $\mathbf{R}$), then there is no interaction between two spin carriers, and we may propagate the two spin degrees of freedom separately (with $\mathbf{h}^{s\uparrow}$ and $\mathbf{h}^{s\downarrow}$). Obviously if there is no spin-orbit interaction, and $\mathbf{h}^{s\uparrow} = \mathbf{h}^{s\downarrow}$, the dynamics of the different spin carriers will be the same. However, when $\mathbf{h}^{s\uparrow} \neq \mathbf{h}^{s\downarrow}$, we will show that substantially different spin currents can arise.

D. Evaluating friction tensors, covariance matrix, and adiabatic force

We will now evaluate Eqs. (2)–(4) for the molecular junction Hamiltonian described by Eqs. (5)–(8).

We begin with the friction tensor. For an arbitrary voltage, Eq. (2) can be further simplified under the Condon approximation where the coupling $V_{p,k\alpha}$ is independent of the nuclear position $\mathbf{R}$. As a result, $\mathcal{H}$ in Eq. (2) can be replaced with h^s. Then $\mathcal{G}$ can be expanded in molecular orbital basis, turning $\mathcal{G}$ into G which is the Green's function of molecule. An analytic expression for the friction tensor for a general two-orbital

Orbital 1

Orbital 2
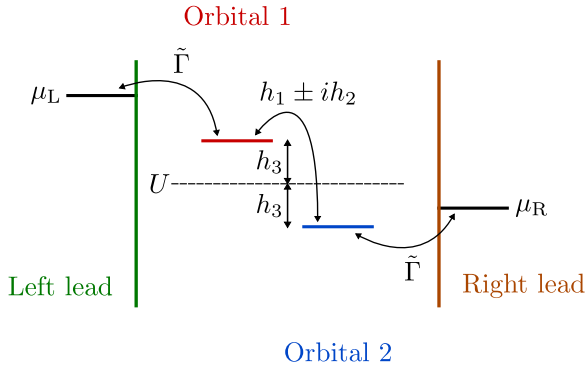
FIG. 1. A schematic picture of our molecular junction model. μ_L and μ_R are chemical potentials of the left and right leads, and the source-drain voltage $V_{sd} = \mu_L - \mu_R$ controls the voltage bias. Other parameters are defined in the text.

two-mode Hamiltonian [namely $\mathbf{h}^{s\uparrow} = \mathbf{h}(x, y) \cdot \boldsymbol{\sigma}$] was derived in Ref. [30] (and see Appendix A); the results are

$$\gamma_{\mu\nu} = \gamma_{\mu\nu}^S + \gamma_{\mu\nu}^A, \tag{12}$$

$$\begin{aligned}\gamma_{\mu\nu}^S = \frac{2}{\pi} \int_{-\infty}^{\infty} d\epsilon \{&-2\text{Re}\{C\tilde{\epsilon}\}(\partial_\mu \mathbf{h} \cdot \partial_\nu \mathbf{h})(\mathbf{h} \cdot \boldsymbol{\kappa}) \\ &+ 2\text{Re}\{C\tilde{\epsilon}\}(\partial_\mu \mathbf{h} \cdot \mathbf{h})(\partial_\nu \mathbf{h} \cdot \boldsymbol{\kappa}) \\ &+ 2\text{Re}\{C\tilde{\epsilon}\}(\partial_\nu \mathbf{h} \cdot \mathbf{h})(\partial_\mu \mathbf{h} \cdot \boldsymbol{\kappa}) \\ &+ \kappa_0 \text{Re}\{C(\tilde{\epsilon}^2 + h^2)\}\partial_\mu \mathbf{h} \cdot \partial_\nu \mathbf{h}\}, \tag{13}\end{aligned}$$

$$\begin{aligned}\gamma_{\mu\nu}^A = \frac{2}{\pi} \int_{-\infty}^{\infty} d\epsilon \{&-\text{Im}\{C(\tilde{\epsilon}^2 + h^2)\}\boldsymbol{\kappa} \cdot (\partial_\mu \mathbf{h} \times \partial_\nu \mathbf{h}) \\ &+ 2\kappa_0 \text{Im}\{C\tilde{\epsilon}\}\mathbf{h} \cdot (\partial_\mu \mathbf{h} \times \partial_\nu \mathbf{h})\}, \tag{14}\end{aligned}$$

where $C \equiv -(\frac{1}{\tilde{\epsilon}^2 - h^2})^2 i\tilde{\Gamma}|\frac{1}{\tilde{\epsilon}^2 - h^2}|^2$ and $\tilde{\epsilon} = \epsilon + i\tilde{\Gamma}/2$ is a complex number. $\tilde{\Gamma}$ represents the molecule-lead coupling strength, which is a constant under the wide-band-limit approximation, i.e., $\tilde{\Gamma} = \Gamma_{11} = \Gamma_{22}$. Here we have defined $\Gamma_{mn} \equiv 2\pi \sum_{k\alpha} V_{m,k\alpha}V_{n,k\alpha}^* \delta(\epsilon - \epsilon_{k\alpha})$; note that the off-diagonal elements Γ_{12} and Γ_{21} are zero because orbital 1 couples only to the left lead and orbital 2 couples only to the right lead. See Fig. 1 for a schematic picture.

The components of $\boldsymbol{\kappa}$ are

$$\kappa_0 = \tfrac{1}{2}\big[(f_L + f_R)(h_1^2 + h_2^2) + f_L|\tilde{\epsilon} + h_3|^2 + f_R|\tilde{\epsilon} - h_3|^2\big],$$

$$\kappa_1 = \text{Re}\{[f_L(\tilde{\epsilon}^* + h_3) + f_R(\tilde{\epsilon} - h_3)](h_1 + ih_2)\},$$

$$\kappa_2 = \text{Im}\{[f_L(\tilde{\epsilon}^* + h_3) + f_R(\tilde{\epsilon} - h_3)](h_1 + ih_2)\},$$

$$\kappa_3 = \tfrac{1}{2}\big[(f_R - f_L)(h_1^2 + h_2^2) + f_L|\tilde{\epsilon} + h_3|^2 - f_R|\tilde{\epsilon} - h_3|^2\big].$$

Notice that all of the κ's are real functions. Also, when the total system is in equilibrium, i.e., when $f_L = f_R = f$,

$$\kappa_0 = f\left(\epsilon^2 + h^2 + \frac{\Gamma^2}{4}\right), \quad \boldsymbol{\kappa} = 2f\epsilon\mathbf{h}.$$

Equations (12)–(14) will be used below to propagate Eq. (1).

Next, we will derive an analytic form for the random force covariance matrix for the two-orbital two-mode system Hamiltonian, $\mathbf{h}^{s\uparrow} = \mathbf{h}(x, y) \cdot \boldsymbol{\sigma}$. As in the case of the friction tensor, if we consider the Condon limit, the trace in Eq. (3) is taken over only the molecular orbitals. Therefore,

$$\begin{aligned}\frac{1}{2}\big(\bar{D}_{\mu\nu}^S + \bar{D}_{\nu\mu}^S\big) = \frac{\hbar}{8\pi} \int_{-\infty}^{\infty} d\epsilon \{&\text{Tr}\{\partial_\mu hG^R(\epsilon)\partial_\nu hG^<(\epsilon)\}. \\ &+ \text{Tr}\{\partial_\nu hG^R(\epsilon)\partial_\mu hG^<(\epsilon)\} \\ &+ \text{Tr}\{\partial_\mu hG^<(\epsilon)\partial_\nu hG^<(\epsilon)\}\} + \text{H.c.} \tag{15}\end{aligned}$$

Here

$$G^R(\epsilon) = \frac{1}{\epsilon - h - \Sigma^R}$$

is the molecule retarded Green's function with Σ^R denoting the molecule retarded self-energy,

$$\Sigma_{mn}^R = \sum_{k\alpha} V_{m,k\alpha}g_{k\alpha}^R V_{k\alpha,n},$$

with $g_{k\alpha}^R = (\epsilon - \epsilon_{k\alpha} + i\eta)^{-1}$ as the lead retarded self-energy; and $G^<(\epsilon)$ is the molecule lesser Green's function.

Now, for our two-orbital two-mode model Hamiltonian, in the standard wide-band-limit approximation, the retarded self-energy becomes $\Sigma^R = -i\tilde{\Gamma}\mathbf{I}_{2\times2}/2$ since the left lead couples only to orbital 1 and the right lead couples only to orbital 2 (as assumed in the calculation of friction tensor). With this simplification, it follows that [30]

$$G^R = \frac{1}{\tilde{\epsilon}^2 - h^2}(\tilde{\epsilon} + \mathbf{h} \cdot \boldsymbol{\sigma}), \tag{16}$$

$$G^< = i\tilde{\Gamma}\left|\frac{1}{\tilde{\epsilon}^2 - h^2}\right|^2 (\kappa_0 + \boldsymbol{\kappa} \cdot \boldsymbol{\sigma}). \tag{17}$$

By using Eqs. (16) and (17), Eq. (15) becomes ($\hbar = 1$)

$$\begin{aligned}\frac{1}{2}\big(\bar{D}_{\mu\nu}^S + \bar{D}_{\nu\mu}^S\big) = \frac{1}{2\pi} \int_{-\infty}^{\infty} d\epsilon \{&-2\text{Re}\{C'\}(\partial_\mu \mathbf{h} \cdot \partial_\nu \mathbf{h})(\mathbf{h} \cdot \boldsymbol{\kappa}) \\ &+ 2\text{Re}\{C'\}(\partial_\mu \mathbf{h} \cdot \mathbf{h})(\partial_\nu \mathbf{h} \cdot \boldsymbol{\kappa}) \\ &+ 2\text{Re}\{C'\}(\partial_\nu \mathbf{h} \cdot \mathbf{h})(\partial_\mu \mathbf{h} \cdot \boldsymbol{\kappa}) \\ &+ 2\kappa_0 \text{Re}\{C'\tilde{\epsilon}\}\partial_\mu \mathbf{h} \cdot \partial_\nu \mathbf{h} \\ &+ C''\big[2(\partial_\mu \mathbf{h} \cdot \boldsymbol{\kappa})(\partial_\nu \mathbf{h} \cdot \boldsymbol{\kappa}) \\ &+ \big(\kappa_0^2 - \kappa^2\big)\partial_\mu \mathbf{h} \cdot \partial_\nu \mathbf{h}\big]\}, \tag{18}\end{aligned}$$

where

$$C' \equiv \left(\frac{1}{\tilde{\epsilon}^2 - h^2}\right)i\tilde{\Gamma}\left|\frac{1}{\tilde{\epsilon}^2 - h^2}\right|^2, \quad C'' \equiv -\tilde{\Gamma}^2\left|\frac{1}{\tilde{\epsilon}^2 - h^2}\right|^4.$$

Equation (18) is the covariance matrix we use for evaluating the random force in practice for propagating the Langevin equation, Eq. (1).

Finally, in our two-orbital model, according to Eq. (17), the adiabatic force Eq. (4) becomes

$$F_\mu = -\frac{\tilde{\Gamma}}{\pi} \int_{-\infty}^{\infty} \left|\frac{1}{\tilde{\epsilon}^2 - h^2}\right|^2 \partial_\mu \mathbf{h} \cdot \boldsymbol{\kappa} - \partial_\mu U.$$

E. Evaluating the current

We describe details of current calculations in this section. Let μ_L and μ_R be the Fermi levels in the left and right leads, with voltage $V \equiv \mu_L - \mu_R$ across the molecule. For the Hamiltonian in Eq. (11), we run Langevin dynamics and calculate the spin current $I^{\uparrow/\downarrow}$ by taking an ensemble average over nuclear DoFs,

$$I^{\uparrow/\downarrow} = \int d\mathbf{R}\, d\mathbf{P}\, I_{\text{loc}}(\mathbf{R})\rho^{\uparrow/\downarrow}(\mathbf{R}, \mathbf{P}). \qquad (19)$$

The nuclear probability density $\rho^{\uparrow/\downarrow}(\mathbf{R}, \mathbf{P})$ is determined by sampling 1000 trajectories, running dynamics according to Eq. (1), and evaluating how many trajectories are at $(\mathbf{R}, \mathbf{P})$ in phase space at steady state. We make the ansatz that the local spin current I_{loc} flowing from the left lead through the molecule to the right lead can be evaluated by the Landauer formula [41]

$$I_{\text{loc}} = \frac{e}{2\pi\hbar} \int_{-\infty}^{\infty} d\epsilon\, T(\epsilon)[f_L(\epsilon) - f_R(\epsilon)], \qquad (20)$$

where $T(\epsilon)$ is the transmission probability that can be expressed in terms of Green's functions (see Ref. [41] or [39] for details):

$$T(\epsilon) = \text{Tr}\{\Gamma^L G^R(\epsilon)\Gamma^R G^A(\epsilon)\}. \qquad (21)$$

Within our setup, only orbital 1 couples to the left lead and only orbital 2 couples to the right lead. Thus, the Γ matrices are

$$\Gamma^L = \begin{pmatrix} \tilde{\Gamma} & 0 \\ 0 & 0 \end{pmatrix}, \quad \Gamma^R = \begin{pmatrix} 0 & 0 \\ 0 & \tilde{\Gamma} \end{pmatrix}.$$

Hence,

$$T(\epsilon) = \tilde{\Gamma}^2 G_{12}^R G_{21}^A = \tilde{\Gamma}^2(h_1^2 + h_2^2)\left|\frac{1}{\tilde{\epsilon}^2 - h^2}\right|^2.$$

Note that $T(\epsilon)$ is invariant to changing $h_2 \to -h_2$, which implies that the local current I_{loc} is in fact independent of the exact spin carrier. For this reason we have not included any superscripts $\uparrow/\downarrow$ in Eqs. (20) and (21).

Note that one cannot distinguish the two spin carriers if the two probability densities $\rho^{\uparrow/\downarrow}$ are the same. Note also that, for the case of a single resonant level, the current calculated by Eq. (19) has been shown to agree with numerically exact HEOM calculations [42].

III. RESULTS

A. Spin polarization

In Fig. 2 we plot the spin current [calculated by utilizing Eq. (19)] and the corresponding spin polarization results in the symmetric case ($\Delta = 0$) with $\mu_L = -\mu_R$. The spin polarization is defined as the standard quantity $(I^{\downarrow} - I^{\uparrow})/(I^{\downarrow} + I^{\uparrow})$. For this initial set of data, we simulate a large SOC; we set $A = B = \chi = 1$ so that the average $\langle Ax \rangle$ is of the same order of magnitude as $\langle By \rangle$. We find an 18% spin polarization; furthermore, we find decaying and the oscillating behaviors in the large bias limit, which is consistent with the magnetic AFM results in Ref. [13].
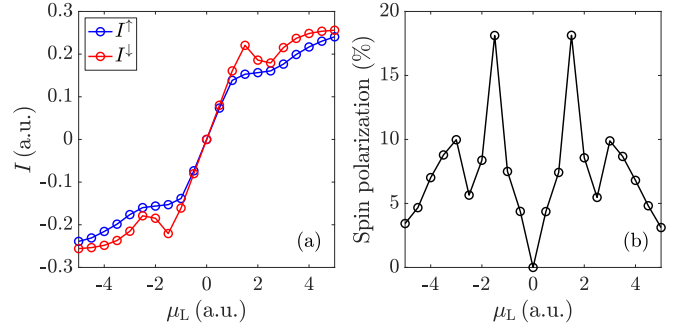
FIG. 2. $\Delta = 0, A = B = 1, \kappa_x = 0, \chi = 1, \kappa_y = 0.8, \tilde{\Gamma} = 1$, and $\mu_L = -\mu_R$. We utilize Eq. (19) to calculate (a) the spin current and (b) the corresponding spin polarization. No spin polarization is predicted when the voltage bias is zero. Sizable spin polarization can be found at finite μ_L. The decaying and the oscillating behaviors at large bias limit are consistent with an AFM CISS experiment.

In Figs. 3(a) and 3(b) we utilize Eq. (19) to calculate the spin currents and the corresponding spin polarization in the presence of a nonzero energy gap $\Delta = 3$ between the two orbitals. Compared to the case $\Delta = 0$, the spin polarization is enhanced for positive μ_L but is diminished for negative μ_L. To date, we have run several calculations for symmetric systems ($\Delta = 0$) and asymmetric systems ($\Delta \neq 0$). In general, we find that spin current results depend sensitively on the global nature of the potential energy surface (and not just the spin-orbit coupling).

In order to illustrate microscopic origins of spin polarization, we consider the asymmetric Hamiltonian (with $\Delta = 3$, $\kappa_x = 0$, and $\kappa_y = 1$). For such a Hamiltonian, a large spin current is found when $\mu_L = -\mu_R = 3.5$. In Figs. 4(c) and 4(d) we plot the antisymmetric friction tensors (corresponding to the pseudomagnetic field) when $B = 1$ and $B = -1$, respectively. The adiabatic ground state potential is plotted in Fig. 4(b). For such a Hamiltonian, one finds very well separated nuclear nonequilibrium steady state distributions in position space $\rho^{\uparrow/\downarrow}(\mathbf{R}, \mathbf{P})$ for different spin carriers as shown in Fig. 4(a) and this separation of nuclear densities leads to different spin currents. To explain why the nuclear steady state densities are so different *out of equilibrium* (even though they must agree at equilibrium), note that the spin up carriers are
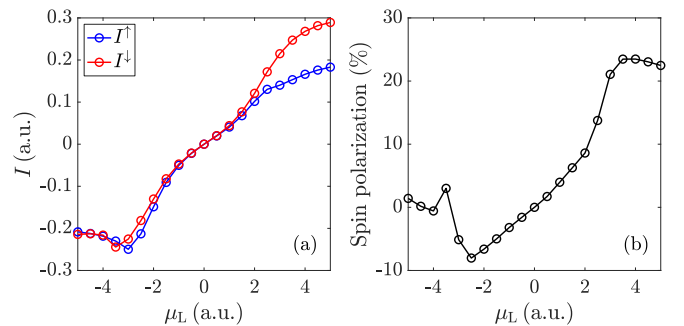
FIG. 3. Calculations for (a) spin currents and (b) the corresponding spin polarization when the voltage bias is nonzero. Parameters: $\Delta = 3, A = B = 1, \kappa_x = 0, \chi = 1$, and $\kappa = 1$. The spin polarization is enhanced when $\Delta \neq 0$.
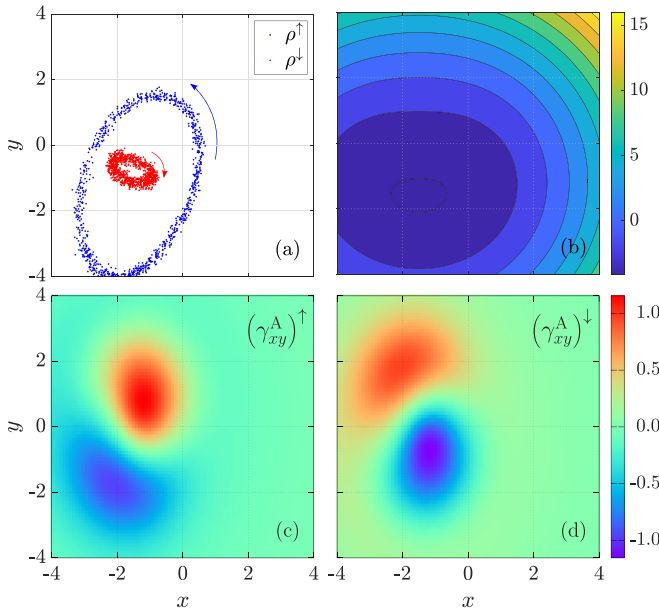
FIG. 4. (a) Scatter plot distribution of spin up/down carriers in steady state with an overall arrow indicating the direction of motion. (b) Adiabatic ground state obtained from diagonalizing $\mathbf{h}^{s\uparrow} + U$. (c) Antisymmetric friction tensor for $B = 1$ (spin up). (d) Antisymmetric friction tensor for $B = -1$ (spin down). The combination of the adiabatic force and the different pseudomagnetic fields for spin up and down leads to different steady state nuclear probability distributions.

affected both by the two opposite pseudomagnetic fields [blue and red regions in Fig. 4(c)] and the (adiabatic) restoring force in Fig. 4(b). As a result, the trajectories trace out the big circulating vector field (with an overall blue arrow indicating the direction of motion) in Fig. 4(a). By contrast, the spin down carriers experience only one kind of pseudomagnetic field [the blue region in Fig. 4(d)] so that their steady state nuclear distribution does not stray far from the equilibrium region [see the red dots in Fig. 4(a)]. This nonequilibrium difference in steady state nuclear distributions leads to clear differences in spin currents. As a side note, the nuclear Berry curvature effect becomes small when the voltage is very large and, in such a case, we predict that a distinction between spins can no longer be achieved. This prediction is in agreement with the AFM-CISS experiment, whereby the difference in current (between systems with up and down magnetic fields) is found to decrease at large voltages [13].

B. Spin polarization for a small spin-orbit coupling

We have not yet formally addressed the question of the size of the spin-orbit interaction. One can ask: can reasonable spin polarization emerge if the spin-orbit interaction is not too large? To answer such a question, in Figs. 6(a) and 6(b) we calculate the spin currents and the corresponding spin polarization with a smaller spin-orbit interaction. More specifically, we reduce both B [in Eq. (9)] and χ [in Eq. (10)]: we set $B = \chi = 0.1$ so that $\langle By \rangle \ll \langle Ax \rangle$. While reducing χ should lead to larger fluctuations in the position y, reducing B leads to a smaller total spin-orbit coupling matrix element. In Fig. 5 we
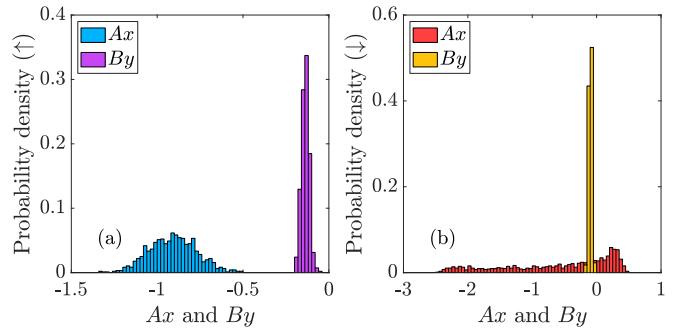
FIG. 5. Probability distribution of Ax and By for (a) spin up (b) spin down carriers.

show a histogram of the resulting diabatic couplings (Ax) and spin-orbit couplings (By); note that indeed we have reduced the total size of the average spin-orbit coupling relative to the average diabatic coupling. In Fig. 6 we then show the resulting currents and spin polarization. Observe that a meaningful spin polarization can indeed be obtained, even when the spin-orbit coupling matrix elements are one tenth the size of the diabatic coupling matrix elements.

IV. CONCLUSION

In conclusion, we have demonstrated that, in the presence of a nonzero electronic current, Berry curvature effects can lead to spin separation of nuclear wave packets and spin polarization of the electronic current. These effects arise because (i) the presence of spin-orbit coupling creates a Berry force that comes from the nonadiabatic effects and does not obey time-reversal symmetry within a master equation model, and (ii) the presence of a finite voltage leads to a random force that does not obey a fluctuation-dissipation theorem. Altogether, these two effects lead to the scenario whereby the steady states for nuclear wave packets with spin up electrons can be very different from the steady states for nuclear wave packets with spin down electrons. Importantly, we find that a sizable spin polarization can be achieved even in the situation where the spin-orbit coupling is small (a tenth of
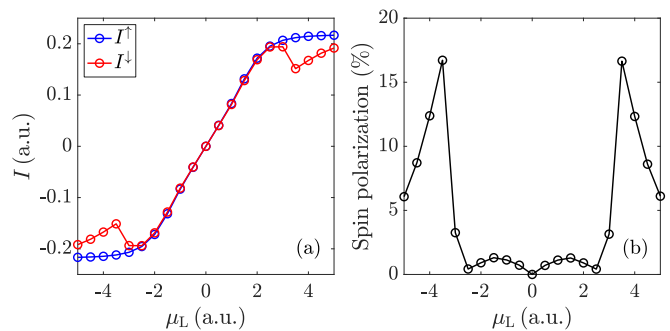
FIG. 6. Calculations for (a) spin currents and (b) the corresponding spin polarization when the spin-orbit coupling is small. Parameters: $\Delta = 0$, $A = 1$, $B = 0.1$, $\kappa_x = 0$, $\chi = 0.1$, and $\kappa = 0.1$. Sizable spin polarization can still be achieved when different mode frequencies are considered.

a diabatic coupling) when modes with different frequencies are considered; future research will be necessary to address exactly how small the spin-orbit coupling can be and still yield a meaningful effect—especially given the possibility of more than two orbitals and possible conical intersections. (Note that our model has made the simplifying approximation that different spin carriers do not mix with each other, and future work will also be necessary to explore the implication of spin-flip processes.) Lastly, our results in Fig. 4 have shown that, as a result of nuclear motion, decaying and oscillating signatures in the polarization can emerge as a function of voltage for the magnetic AFM setup (which has been observed experimentally [13]).

Looking forward, there are many questions that must be addressed. First and most importantly, the model presented here is clearly just a model: in the future, one would like to run fully *ab initio* dynamics without any parameters. Second, the strong dependence of the spin current on the U term in Eq. (10) is interesting and highlights the fact that, if electronic spin transitions are coupled to nuclear dynamics, then understanding spin dynamics may necessarily require modeling the full totality of chemical dynamics; spin-orbit coupling will not be the only determinant of spin current. In fact, optimizing spin polarization in practice (experimentally) might require optimizing nuclear barriers (rather than just increasing SOC). Third, in this article we have focused explicitly on systems with only two orbitals, and for such a system, one cannot extract a spin current without nuclear motion. However, if we allow for three or more orbitals (and freeze the nuclei), one can extract different (but small) spin currents based on purely electronic considerations. How will the spin polarization based on nuclear nonadiabatic motion scale with system size, especially if we were to treat a true helix? Note that CISS experiments on DNA are very sensitive to the length of the DNA [43]. There are many exciting questions to answer in the future.

Altogether, the present article suggests that a merger of spintronics and nonadiabatic dynamics is on the horizon, and the experimental observation of nonequilibrium spin separation and polarization in chemical systems would appear to be the glue that connects together these two titanic fields of condensed matter physics.

ACKNOWLEDGMENTS

APPENDIX A: A BRIEF REVIEW OF THE FOKKER-PLANCK EQUATION WITH ELECTRONIC FRICTION

In this Appendix we will briefly review the friction tensor $\gamma_{\mu\nu}$ in Eq. (1) in the main body of the text. The equation of motion driving the nuclear probability density $\rho(\mathbf{R}, \mathbf{P})$ (for notational simplicity here we consider the spinless case) can be derived from the mixed quantum-classical Liouville equation [44] followed by the Mori-Zwanzig method and the

adiabatic approximation [34],

$$\partial_t \rho = -\sum_\mu \frac{P_\mu}{m_\mu} \partial_\mu \rho - \sum_\mu F_\mu \frac{\partial \rho}{\partial P_\mu} + \sum_{\mu\nu} \gamma_{\mu\nu} \frac{\partial}{\partial P_\mu} \left(\frac{P_\nu}{m_\nu} \rho \right) + \sum_{\mu\nu} \bar{D}^{\mathrm{S}}_{\mu\nu} \frac{\partial^2 \rho}{\partial P_\mu \partial P_\nu}. \tag{A1}$$

For this Fokker-Planck equation, which is equivalent to Eq. (1), the adiabatic force F_μ, friction tensor $\gamma_{\mu\nu}$, and covariance matrix $\bar{D}^{\mathrm{S}}_{\mu\nu}$ for the random force ζ_μ [in Eq. (1)] are [34]

$$F_\mu = -\mathrm{Tr}\{\partial_\mu \hat{H} \hat{\rho}_{\mathrm{ss}}\}, \tag{A2}$$

$$\gamma_{\mu\nu} = -\int_0^\infty dt\, \mathrm{Tr}\{\partial_\mu \hat{H} e^{-i\hat{H}t/\hbar} \partial_\nu \hat{\rho}_{\mathrm{ss}} e^{i\hat{H}t/\hbar}\}, \tag{A3}$$

$$\bar{D}^{\mathrm{S}}_{\mu\nu} = \frac{1}{2} \int_0^\infty dt\, \mathrm{Tr}\{e^{i\hat{H}t/\hbar} \delta\hat{F}_\mu e^{-i\hat{H}t/\hbar} (\delta\hat{F}_\nu \hat{\rho}_{\mathrm{ss}} + \hat{\rho}_{\mathrm{ss}} \delta\hat{F}_\nu)\}, \tag{A4}$$

$$\delta\hat{F}_\mu = -\partial_\mu \hat{H} + \mathrm{Tr}\{\partial_\mu \hat{H} \hat{\rho}_{\mathrm{ss}}\}. \tag{A5}$$

Note that $\bar{D}^{\mathrm{S}}_{\mu\nu} \neq \bar{D}^{\mathrm{S}}_{\nu\mu}$, but the antisymmetric part of $\bar{D}^{\mathrm{S}}$ does not contribute to the EOM in Eq. (A1). Thus, we calculate only symmetrized $\bar{D}^{\mathrm{S}}$ in the main body of the text. Here $\hat{H}$ is the electronic Hamiltonian, $\hat{\rho}_{\mathrm{ss}}$ is the steady state density matrix satisfying $[\hat{H}, \hat{\rho}_{\mathrm{ss}}] = 0$, and $\bar{D}^{\mathrm{S}}_{\mu\nu}$ is in the Markovian limit such that the random force $\zeta_\mu(t)$ satisfies the time correlation function,

$$\tfrac{1}{2}[\langle \zeta_\mu(t)\zeta_\nu(t') \rangle + \langle \zeta_\nu(t)\zeta_\mu(t') \rangle] = \bar{D}^{\mathrm{S}}_{\mu\nu} \delta(t - t').$$

Using these well-established expressions from Ref. [34], we will now derive Eqs. (2)–(4) in the main body of the text.

1. The friction tensor

When a noninteracting Hamiltonian $\hat{H} = \sum_{pq} \mathcal{H}_{pq}(\mathbf{R}) \hat{d}^\dagger_p \hat{d}_q + U(\mathbf{R})$ is considered [$\hat{d}^\dagger_p$ ($\hat{d}_p$) creates (annihilates) an electron in orbital p, and $U(\mathbf{R})$ is a purely nuclear potential energy], the friction tensor becomes [45]

$$\gamma_{\mu\nu} = -\frac{1}{2\pi} \int_{-\infty}^\infty d\epsilon\, \mathrm{Tr}\{\partial_\mu \mathcal{H} \mathcal{G}^{\mathrm{R}} \partial_\nu \sigma_{\mathrm{ss}} \mathcal{G}^{\mathrm{A}}\},$$

where $\mathcal{G}^{\mathrm{R/A}} = (\epsilon - \mathcal{H} \pm i\eta)^{-1}$ is the retarded/advanced Green's function of the electron, and

$$\sigma^{\mathrm{ss}}_{qp} \equiv \mathrm{Tr}\{\hat{\rho}_{\mathrm{ss}} \hat{d}^\dagger_p \hat{d}_q\} = \int_{-\infty}^\infty \frac{d\epsilon}{2\pi i} \mathcal{G}^<_{qp}(\epsilon). \tag{A6}$$

Here $\mathcal{G}^<_{qp}(\epsilon)$ is the lesser Green's function in the energy domain. Here we have used the fact that $\mathcal{G}^<_{qp}(t_1, t_2) = \mathcal{G}^<_{qp}(t_2 - t_1)$, due to $[\hat{H}, \hat{\rho}_{\mathrm{ss}}] = 0$, so that the conventional time-domain lesser Green's function

$$\mathcal{G}^<_{qp}(t_1, t_2) \equiv \frac{i}{\hbar} \mathrm{Tr}\{\hat{\rho}_{\mathrm{ss}} \hat{d}^\dagger_p(t_2) \hat{d}_q(t_1)\}$$

can be Fourier transformed.

In order to proceed, $\mathcal{G}^<(\epsilon)$ is constructed to follow the Keldysh equation $\mathcal{G}^< = \mathcal{G}^{\mathrm{R}} \Pi^< \mathcal{G}^{\mathrm{A}}$ (this is true when the relaxation from the system described by $\hat{H}$ to a fictitious outer bath is fast enough [45]) where $\Pi^<$ is the electron lesser self-energy assumed to be independent of ϵ. Then the friction

tensor $\gamma_{\mu\nu}$ becomes [45]

$$\gamma_{\mu\nu} = \frac{\hbar}{2\pi} \int_{-\infty}^{\infty} d\epsilon \, \text{Tr}\{\partial_\mu \mathcal{H} \partial_\epsilon \mathcal{G}^R \partial_\nu \mathcal{H} \mathcal{G}^<\} + \text{H.c.} \quad (A7)$$

This is Eq. (2) above. Using Eq. (A7) and Eqs. (16) and (17), one can derive Eqs. (13) and (14).

In equilibrium, as shown in Ref. [30], the antisymmetric part of Eq. (A7) can be simplified. The result is

$$\gamma_{\mu\nu}^A \propto - \sum_{k \neq l, \epsilon_k \neq \epsilon_l} 2\text{Im}\{d_{kl}^\mu d_{lk}^\nu\}[f(\epsilon_k) - f(\epsilon_l)], \quad (A8)$$

where $d_{kl}^\mu \equiv \langle k|\partial_\mu|l\rangle$ is the derivative coupling between Lehmann representations, and $f(\epsilon) = 1/\{\exp[\beta(\epsilon - \mu)] + 1\}$ represents Fermi-Dirac distribution. We emphasize that Eq. (A8) is valid only in equilibrium.

2. The adiabatic force

Next, let us turn to the adiabatic force. As has been discussed at great length, such a force is nonconservative out of equilibrium in the presence of a current. In order to calculate such a force in Eq. (A2), we plug Eq. (A6) into Eq. (A2),

$$F_\mu = - \sum_{pq} \mathcal{H}_{pq}(\mathbf{R})\sigma_{qp}^{\text{ss}} - \partial_\mu U(\mathbf{R})$$

$$= -\frac{1}{2\pi i} \int_{-\infty}^{\infty} d\epsilon \, \text{Tr}\{\partial_\mu \mathcal{H} \mathcal{G}^<\} - \partial_\mu U.$$

We further make the Condon approximation such that only the system Hamiltonian (rather than the system-bath Hamiltonian) changes as a function of a nuclear coordinate:

$$F_\mu = -\frac{1}{2\pi i} \int_{-\infty}^{\infty} d\epsilon \, \text{Tr}\{\partial_\mu h G^<\} - \partial_\mu U. \quad (A9)$$

This is Eq. (4) above. In practice, above we evaluated Eq. (A9) numerically with Eqs. (13) and (14).

3. The covariance $\bar{D}_{\mu\nu}^{\text{S}}$

Equations (2) and (4) above are not new. However, to our knowledge, no one has yet presented a formal expression for the covariance of the random force under nonequilibrium conditions for a complex-valued Hamiltonian. We will do so now. To proceed, we first note that when a noninteracting Hamiltonian is considered, $U(\mathbf{R})$ does not contribute to $\delta\hat{F}_\mu$, since according to Eq. (A5),

$$\delta\hat{F}_\mu = -\sum_{pq} \partial_\mu \mathcal{H}_{pq}(\hat{d}_p^\dagger \hat{d}_q - \sigma_{qp}^{\text{ss}}). \quad (A10)$$

Furthermore, since $U(\mathbf{R})$ is a scalar function, it does not contribute to $\bar{D}_{\mu\nu}^{\text{S}}$ according to Eq. (A4). Second, according to Eq. (A4), $\bar{D}_{\mu\nu}^{\text{S}}$ consists of two parts involving $\delta\hat{F}_\nu \hat{\rho}_{\text{ss}}$ and $\hat{\rho}_{\text{ss}}\delta\hat{F}_\nu$, respectively, and the two parts are Hermitian conjugate to each other. We focus on the former and substitute Eq. (A10)

for $\delta\hat{F}_\mu$ in Eq. (A4):

$$\frac{1}{2} \int_0^\infty dt \, \text{Tr}\{e^{i\hat{H}t/\hbar} \delta\hat{F}_\mu e^{-i\hat{H}t/\hbar} \delta\hat{F}_\nu \hat{\rho}_{\text{ss}}\}$$

$$= \frac{1}{2} \int_0^\infty dt \, \text{Tr}\left\{ e^{i\hat{H}t/\hbar} \sum_{pq} \partial_\mu \mathcal{H}_{pq} (\hat{d}_p^\dagger \hat{d}_q - \sigma_{qp}^{\text{ss}}) e^{-i\hat{H}t/\hbar} \right.$$

$$\left. \times \sum_{rs} \partial_\nu \mathcal{H}_{rs} (\hat{d}_r^\dagger \hat{d}_s - \sigma_{sr}^{\text{ss}}) \hat{\rho}_{\text{ss}} \right\}$$

$$= \frac{1}{2} \int_0^\infty dt \, \text{Tr}\{\partial_\mu \mathcal{H} e^{-i\mathcal{H}t/\hbar}(1 - \sigma^{\text{ss}}) \partial_\nu \mathcal{H} \sigma^{\text{ss}} e^{i\mathcal{H}t/\hbar}\}.$$

Here we have utilized Wick's theorem to evaluate a two particle Green's function $\text{Tr}\{\hat{d}_a^\dagger \hat{d}_b \hat{d}_r^\dagger \hat{d}_s \hat{\rho}_{\text{ss}}\}$ (see Eqs. (5.1) and (5.27) in Ref. [46]),

$$\text{Tr}\{\hat{\rho}_{\text{ss}} \hat{d}_a^\dagger(4) \hat{d}_b(3) \hat{d}_r^\dagger(2) \hat{d}_s(1)\}$$

$$= -\text{Tr}\{\mathcal{T}[\hat{\rho}_{\text{ss}} \hat{d}_b(3) \hat{d}_s(1) \hat{d}_a^\dagger(4) \hat{d}_r^\dagger(2)]\}$$

$$= G_2(3, 1; 2, 4)$$

$$= \sigma_{sa}^{\text{ss}}(\delta_{br} - \sigma_{br}^{\text{ss}}) + \sigma_{ba}^{\text{ss}}\sigma_{sr}^{\text{ss}}.$$

We proceed to write Eq. (A4) in the energy domain,

$$\bar{D}_{\mu\nu}^{\text{S}} = \frac{\hbar}{4\pi} \int_{-\infty}^{\infty} d\epsilon \, \text{Tr}\left\{ \partial_\mu \mathcal{H} \frac{1}{\epsilon - \mathcal{H} + i\eta}(1 - \sigma^{\text{ss}}) \partial_\nu \mathcal{H} \sigma^{\text{ss}} \right.$$

$$\left. \times \frac{1}{\epsilon - \mathcal{H} - i\eta} \right\} + \text{H.c.}, \quad (A11)$$

where we have used integral representations of the Dirac delta function and the Heaviside function.

In order to evaluate $\bar{D}_{\mu\nu}^{\text{S}}$ in practice, we hope to express Eq. (A11) in terms of Green's functions. We expand Eq. (A11) in an orbital basis and utilize the residue theorem to evaluate the integral over ϵ, obtaining

$$\bar{D}_{\mu\nu}^{\text{S}} = i\frac{\hbar}{2} \sum_{pqrs} (\partial_\mu \mathcal{H})_{pq} \frac{1}{\epsilon_p - \epsilon_q + i\eta}(1 - \sigma^{\text{ss}})_{qr}(\partial_\nu \mathcal{H})_{rs}\sigma_{sp}^{\text{ss}}$$

$$+ \text{H.c.} \quad (A12)$$

Then we replace σ^{ss} by using Eq. (A6). Next, we further assume that the relaxation from the system modeled by $\hat{H}$ (more specifically from the bath Hamiltonian $\hat{H}_b$) as caused by a fictitious outer bath is fast enough so that we can utilize the Keldysh relation,

$$\mathcal{G}^<(\epsilon) = \mathcal{G}^R(\epsilon)\Pi^<\mathcal{G}^A(\epsilon), \quad (A13)$$

where the lesser self-energy is again assumed to be independent of ϵ. As a result, Eq. (A6) becomes

$$\sigma_{qr}^{\text{ss}} \simeq \frac{1}{2\pi i} \int_{-\infty}^{\infty} d\epsilon \, [\mathcal{G}^R(\epsilon)\Pi^<\mathcal{G}^A(\epsilon)]_{qr} = \frac{1}{\epsilon_r - \epsilon_q + i\eta}\Pi_{qr}^<.$$

Note that there are two contributions in Eq. (A12): one with δ_{qr} and the other with σ_{qr}^{ss}. We first address the former,

$$i\frac{\hbar}{2}\sum_{pqrs}(\partial_\mu\mathcal{H})_{pq}\frac{1}{\epsilon_p-\epsilon_q+i\eta}\delta_{qr}(\partial_\nu\mathcal{H})_{rs}\sigma_{sp}^{ss}+\text{H.c.}$$

$$=i\frac{\hbar}{2}\sum_{pqs}(\partial_\mu\mathcal{H})_{pq}\frac{1}{\epsilon_p-\epsilon_q+i\eta}(\partial_\nu\mathcal{H})_{qs}\frac{1}{\epsilon_p-\epsilon_s+i\eta}\Pi_{sp}^<+\text{H.c.}$$

$$=\frac{\hbar}{4\pi}\int_{-\infty}^{\infty}d\epsilon\sum_{pqs}(\partial_\mu\mathcal{H})_{pq}\frac{1}{\epsilon-\epsilon_q+i\eta}(\partial_\nu\mathcal{H})_{qs}\frac{1}{\epsilon-\epsilon_s+i\eta}\Pi_{sp}^<\frac{1}{\epsilon-\epsilon_p-i\eta}+\text{H.c.}$$

$$=\frac{\hbar}{4\pi}\int_{-\infty}^{\infty}d\epsilon\,\text{Tr}\{\partial_\mu\mathcal{H}\mathcal{G}^R(\epsilon)\partial_\nu\mathcal{H}\mathcal{G}^<(\epsilon)\}+\text{H.c.} \tag{A14}$$

Notice that the assumption that $\Pi^<$ is independent of ϵ is necessary for the equality from the second line to the third line. Second, we focus on the latter,

$$-i\frac{\hbar}{2}\sum_{pqrs}(\partial_\mu\mathcal{H})_{pq}\frac{1}{\epsilon_p-\epsilon_q+i\eta}\sigma_{qr}^{ss}(\partial_\nu\mathcal{H})_{rs}\sigma_{sp}^{ss}+\text{H.c.}$$

$$=-i\frac{\hbar}{2}\sum_{pqrs}(\partial_\mu\mathcal{H})_{pq}\frac{1}{\epsilon_p-\epsilon_q+i\eta}\frac{1}{\epsilon_r-\epsilon_q+i\eta}\Pi_{qr}^<(\partial_\nu\mathcal{H})_{rs}\frac{1}{\epsilon_p-\epsilon_s+i\eta}\Pi_{sp}^<+\text{H.c.}$$

$$=-\frac{\hbar}{4\pi}\int_{-\infty}^{\infty}d\epsilon\sum_{pqrs}(\partial_\mu\mathcal{H})_{pq}\frac{1}{\epsilon-\epsilon_q+i\eta}\frac{1}{\epsilon_r-\epsilon_q+i\eta}\Pi_{qr}^<(\partial_\nu\mathcal{H})_{rs}\frac{1}{\epsilon-\epsilon_s+i\eta}\Pi_{sp}^<\frac{1}{\epsilon-\epsilon_p-i\eta}+\text{H.c.}$$

$$=-\frac{\hbar}{4\pi}\int_{-\infty}^{\infty}d\epsilon\sum_{pqrs}(\partial_\mu\mathcal{H})_{pq}\frac{1}{\epsilon_q-\epsilon-i\eta}\Pi_{qr}^<\frac{1}{\epsilon_q-\epsilon_r-i\eta}(\partial_\nu\mathcal{H})_{rs}[\mathcal{G}^<(\epsilon)]_{sp}+\text{H.c.}$$

$$=-i\frac{\hbar}{8\pi^2}\int_{-\infty}^{\infty}d\epsilon\int_{-\infty}^{\infty}d\epsilon'\sum_{pqrs}(\partial_\mu\mathcal{H})_{pq}\frac{1}{\epsilon'-\epsilon-i\eta}\frac{1}{\epsilon'-\epsilon_q+i\eta}\Pi_{qr}^<\frac{1}{\epsilon'-\epsilon_r-i\eta}(\partial_\nu\mathcal{H})_{rs}[\mathcal{G}^<(\epsilon)]_{sp}+\text{H.c.}$$

$$=-i\frac{\hbar}{8\pi^2}\int_{-\infty}^{\infty}d\epsilon\int_{-\infty}^{\infty}d\epsilon'\frac{1}{\epsilon'-\epsilon-i\eta}\text{Tr}\{\partial_\mu\mathcal{H}\mathcal{G}^<(\epsilon')\partial_\nu\mathcal{H}\mathcal{G}^<(\epsilon)\}+\text{H.c.} \tag{A15}$$

Recall that only the "symmetric" part of $\bar{D}_{\mu\nu}^S$ is meaningful in the Fokker-Planck equation, Eq. (A1). Therefore, it is proper to symmetrize Eq. (A15),

$$=-\frac{i}{2}\frac{\hbar}{8\pi^2}\int_{-\infty}^{\infty}d\epsilon\int_{-\infty}^{\infty}d\epsilon'\left(\frac{1}{\epsilon'-\epsilon-i\eta}+\frac{1}{\epsilon-\epsilon'-i\eta}\right)\text{Tr}\{\partial_\mu\mathcal{H}\mathcal{G}^<(\epsilon')\partial_\nu\mathcal{H}\mathcal{G}^<(\epsilon)\}+\text{H.c.}$$

$$=\frac{\hbar}{8\pi}\int_{-\infty}^{\infty}d\epsilon\,\text{Tr}\{\partial_\mu\mathcal{H}\mathcal{G}^<(\epsilon)\partial_\nu\mathcal{G}^<(\epsilon)\}+\text{H.c.} \tag{A16}$$

We must also symmetrize Eq. (A14). If we do so and add up both contributions, we obtain the final result:

$$\frac{1}{2}(\bar{D}_{\mu\nu}^S+\bar{D}_{\nu\mu}^S)=\frac{\hbar}{8\pi}\int_{-\infty}^{\infty}d\epsilon\{\text{Tr}\{\partial_\mu\mathcal{H}\mathcal{G}^R(\epsilon)\partial_\nu\mathcal{H}\mathcal{G}^<(\epsilon)\}+\text{Tr}\{\partial_\nu\mathcal{H}\mathcal{G}^R(\epsilon)\partial_\mu\mathcal{H}\mathcal{G}^<(\epsilon)\}+\text{Tr}\{\partial_\mu\mathcal{H}\mathcal{G}^<(\epsilon)\partial_\nu\mathcal{H}\mathcal{G}^<(\epsilon)\}\}+\text{H.c.} \tag{A17}$$

This is Eq. (3) above.

APPENDIX B: POSITIVE DEFINITENESS OF $(\bar{D}_{\mu\nu}^S+\bar{D}_{\nu\mu}^S)/2$

In this Appendix we prove that the symmetrized covariance matrix $(\bar{D}_{\mu\nu}^S+\bar{D}_{\nu\mu}^S)/2$ is positive definite for a complex-valued Hamiltonian when the system is in/out of equilibrium. This property enables us to utilize the Cholesky decomposition to sample the random force. We start by noticing that, since $[\hat{H},\hat{\rho}_{ss}]=0$, we can always choose a unique Lehmann representation as an eigenbasis for both $\hat{H}$ and $\hat{\rho}_{ss}$, namely $\hat{H}|m\rangle=E_m|m\rangle$ and $\hat{\rho}_{ss}|m\rangle=\rho_m|m\rangle$. (Note that $\rho_m>0$ because a density matrix is positive definite.) Under this representation, the general expression for the covariance matrix $\bar{D}_{\mu\nu}^S$ in Eq. (A4) becomes

$$\bar{D}_{\mu\nu}^S=\frac{i\hbar}{2}\sum_{mn}\frac{1}{E_n-E_m+i\eta}\langle n|\delta\hat{F}_\mu|m\rangle\langle m|\delta\hat{F}_\nu|n\rangle(\rho_m+\rho_n),$$

where we have used integral representations of the Dirac delta function and the Heaviside function. We then symmetrize the covariance matrix,

$$
\frac{1}{2}\left(\bar{D}^{S}_{\mu\nu} + \bar{D}^{S}_{\nu\mu}\right) = \frac{i\hbar}{2} \sum_{mn} \frac{1}{E_n - E_m + i\eta} (\langle n|\delta\hat{F}_{\mu}|m\rangle\langle m|\delta\hat{F}_{\nu}|n\rangle + \langle n|\delta\hat{F}_{\nu}|m\rangle\langle m|\delta\hat{F}_{\mu}|n\rangle)(\rho_m + \rho_n)
$$

$$
= \frac{i\hbar}{2} \sum_{mn} \left(\frac{1}{E_n - E_m + i\eta} + \frac{1}{E_m - E_n + i\eta}\right)\langle n|\delta\hat{F}_{\mu}|m\rangle\langle m|\delta\hat{F}_{\nu}|n\rangle(\rho_m + \rho_n)
$$

$$
= \pi\hbar \sum_{mn} \delta(E_n - E_m)\langle n|\delta\hat{F}_{\mu}|m\rangle\langle m|\delta\hat{F}_{\nu}|n\rangle(\rho_m + \rho_n),
$$

where we have used the representation of the Dirac delta function $\lim_{\epsilon\to0}\epsilon/\pi(x^2 + \epsilon^2) = \delta(x)$. Thus, for arbitrary real vectors $\mathbf{X} \neq 0$, we have

$$
\sum_{\mu\nu} X_{\mu}\frac{1}{2}\left(\bar{D}^{S}_{\mu\nu} + \bar{D}^{S}_{\nu\mu}\right)X_{\nu} = \pi\hbar \sum_{mn} \delta(E_n - E_m)(\rho_m + \rho_n)\left|\langle n|\left(\sum_{\mu} X_{\mu}\delta\hat{F}_{\mu}\right)|m\rangle\right|^2 > 0.
$$

Hence we have proven that $(\bar{D}^{S}_{\mu\nu} + \bar{D}^{S}_{\nu\mu})/2$ is always positive definite.

APPENDIX C: FLUCTUATION-DISSIPATION THEOREM (NONINTERACTING HAMILTONIAN)

In this Appendix we will prove that at equilibrium the fluctuation-dissipation theorem is still obeyed between $\gamma^{S}_{\mu\nu}$ and $(\bar{D}^{S}_{\mu\nu} + \bar{D}^{S}_{\nu\mu})/2$ which is derived in Appendix A 3. Equation (A17) can be recast into a simpler form by using the relation $\mathcal{G}^{R} - \mathcal{G}^{A} = \mathcal{G}^{>} - \mathcal{G}^{<}$,

$$
\frac{1}{2}\left(\bar{D}^{S}_{\mu\nu} + \bar{D}^{S}_{\nu\mu}\right) = \frac{\hbar}{8\pi} \int_{-\infty}^{\infty} d\epsilon\, \mathrm{Tr}\{\partial_{\mu}\mathcal{H}\mathcal{G}^{>}\partial_{\nu}\mathcal{H}\mathcal{G}^{<}\} + \mathrm{H.c.},
$$

which can be further simplified when $\mathcal{G}^{<}$ is anti-Hermitian,

$$
\frac{1}{2}\left(\bar{D}^{S}_{\mu\nu} + \bar{D}^{S}_{\nu\mu}\right) = \frac{\hbar}{4\pi} \int_{-\infty}^{\infty} d\epsilon\, \mathrm{Tr}\{\partial_{\mu}\mathcal{H}\mathcal{G}^{>}\partial_{\nu}\mathcal{H}\mathcal{G}^{<}\}.
$$

Note that in equilibrium $\mathcal{G}^{<}$ is anti-Hermitian because $\mathcal{G}^{<} = -f(\mathcal{G}^{R} - \mathcal{G}^{A})$. Next, we symmetrize Eq. (A7) and consider the equilibrium situation,

$$
\gamma^{S}_{\mu\nu} = \frac{\hbar}{4\pi} \int_{-\infty}^{\infty} d\epsilon\, \mathrm{Tr}\{\partial_{\mu}\mathcal{H}\partial_{\epsilon}\mathcal{G}^{R}\partial_{\nu}\mathcal{H}\mathcal{G}^{<}\} + (\mu \leftrightarrow \nu) + \mathrm{H.c.}
$$

$$
= -\frac{\hbar}{4\pi} \int_{-\infty}^{\infty} d\epsilon\, \mathrm{Tr}\{\partial_{\mu}\mathcal{H}\mathcal{G}^{R}\partial_{\nu}\mathcal{H}\partial_{\epsilon}\mathcal{G}^{<}\} + (\mu \leftrightarrow \nu) + \mathrm{H.c.}
$$

$$
= \frac{\hbar}{4\pi} \int_{-\infty}^{\infty} d\epsilon\, \{\mathrm{Tr}\{\partial_{\mu}\mathcal{H}\mathcal{G}^{R}\partial_{\nu}\mathcal{H}(\mathcal{G}^{R} - \mathcal{G}^{A})\}\partial_{\epsilon}f + \mathrm{Tr}\{\partial_{\mu}\mathcal{H}\mathcal{G}^{R}\partial_{\nu}\mathcal{H}\partial_{\epsilon}(\mathcal{G}^{R} - \mathcal{G}^{A})\}f\} + (\mu \leftrightarrow \nu) + \mathrm{H.c.}
$$

$$
= \frac{\hbar}{4\pi} \int_{-\infty}^{\infty} d\epsilon\, \mathrm{Tr}\{\partial_{\mu}\mathcal{H}(\mathcal{G}^{R} - \mathcal{G}^{A})\partial_{\nu}\mathcal{H}(\mathcal{G}^{R} - \mathcal{G}^{A})\}\partial_{\epsilon}f
$$

$$
= \frac{\beta\hbar}{4\pi} \int_{-\infty}^{\infty} d\epsilon\, \mathrm{Tr}\{\partial_{\mu}\mathcal{H}\mathcal{G}^{>}\partial_{\nu}\mathcal{H}\mathcal{G}^{<}\}
$$

$$
= \beta\frac{1}{2}\left(\bar{D}^{S}_{\mu\nu} + \bar{D}^{S}_{\nu\mu}\right). \tag{C1}
$$

Thus, the fluctuation-dissipation theorem is satisfied at equilibrium.

With the aid of Eq. (C1), one can determine the steady state density distribution using only F_{μ} (and without knowledge of $\gamma_{\mu\nu}$ or $\bar{D}^{S}_{\mu\nu}$). To prove this fact, we need only show that the simplest Boltzmann distribution guess for ρ,

$$
\rho = \frac{e^{-\beta[V(\mathbf{R}) + \sum_{\alpha} P_{\alpha}^2/2m_{\alpha}]}}{Z}, \tag{C2}
$$

satisfies $\partial_t\rho = 0$ [see Eq. (A1)]. Here Z is the partition function. We simply plug Eq. (C2) into the right-hand side of Eq. (A1). The third term becomes

$$
\sum_{\mu\nu} \gamma_{\mu\nu} \frac{\partial}{\partial P_{\mu}}\left(\frac{P_{\nu}}{m_{\nu}}\rho\right) = \sum_{\mu\nu} \gamma^{S}_{\mu\nu} \frac{\partial}{\partial P_{\mu}}\left(\frac{P_{\nu}}{m_{\nu}}\rho\right) + \sum_{\mu\nu} \gamma^{A}_{\mu\nu}\left[\frac{\rho}{m_{\nu}}\delta_{\mu\nu} - \beta\rho\frac{P_{\mu}P_{\nu}}{m_{\mu}m_{\nu}}\right] = \sum_{\mu\nu} \gamma^{S}_{\mu\nu} \frac{\partial}{\partial P_{\mu}}\left(\frac{P_{\nu}}{m_{\nu}}\rho\right).
$$

According to the fluctuation-dissipation theorem in Eq. (C1), the fourth term on the right-hand side of Eq. (A1) becomes

$$\sum_{\mu\nu} \frac{1}{2}\left(\bar{D}^S_{\mu\nu} + \bar{D}^S_{\nu\mu}\right) \frac{\partial^2 \rho}{\partial P_\mu \partial P_\nu} = \sum_{\mu\nu} \frac{\gamma^S_{\mu\nu}}{\beta} \frac{\partial}{\partial P_\mu}\left(-\beta\rho\frac{P_\nu}{m_\nu}\right),$$

which cancels with the third term. (Recall that, as mentioned in Appendix A 3, the antisymmetric part of $\bar{D}^S_{\mu\nu}$ does not enter the Fokker-Planck equation because $\partial^2 \rho / \partial P_\mu \partial P_\nu$ is symmetric.) Also, the first and the second terms on the right-hand side cancel with each other,

$$-\sum_\mu \frac{P_\mu}{m_\mu}\partial_\mu\rho - \sum_\mu F_\mu \frac{\partial\rho}{\partial P_\mu} = -\sum_\mu \frac{P_\mu}{m_\mu}\rho(-\beta)\partial_\mu V - \sum_\mu (-\partial_\mu V)\rho(-\beta)\frac{P_\mu}{m_\mu} = 0.$$

Thus, the Boltzmann distribution is a steady state solution ($\partial_t \rho = 0$). In other words, at equilibrium (where fluctuation dissipation holds), one can use F_μ alone to obtain the steady state probability distribution. However, out of equilibrium, there is no such guarantee and, in the main body of the paper, we show that when there is a current present, ρ can depend critically on $\gamma_{\mu\nu}$ [and be very different for $(\gamma^A_{\mu\nu})^{\uparrow/\downarrow}$].

APPENDIX D: PARAMETERS FOR THE SHIFTED PARABOLA MODEL

The parameters used for the Hamiltonian in Eq. (9) correspond roughly to the *ab initio* parameters extracted for a diphenylmethane junction where we considered the LUMO and LUMO+1 (Sec. J of the SM Ref. [30]). In particular, there we used linear functions $\lambda x + \Delta$ and $Ax + C$ to fit the site energy and real part of the diabatic coupling of the *ab initio* data, respectively; we extracted the parameters $\lambda = 3.44 \times 10^{-4}$, $\Delta = -1.13 \times 10^{-4}$, $A = 3.44 \times 10^{-4}$, and $C = 1.11 \times 10^{-3}$ (all in atomic units). The coupling constant $\tilde{\Gamma}$ is chosen to range over standard values found in the literature (10–100 meV) [15,47,48]. By renormalizing all of the energies above with λ, one finds parameters that are consistent with the parameters used in this article. The only variable that was not extracted in an *ab initio* fashion is the spin-orbit coupling, which was difficult to assess from a small cluster calculation. Thus, above, we have explored the parameter region $B = 0.1$–$1A$ so that we can assess the form of dynamics as B gets smaller.

APPENDIX E: BLOCK DIAGONALIZATION OF TWO-ORBITAL TWO-SPIN HAMILTONIANS

In this Appendix we derive Eq. (11) in more detail. We first consider the following general model Hamiltonian with spin-orbit interaction:

$$H = H_0 + H_{\mathrm{SOC}},$$

where H_0 is a function of only orbital degrees of freedom (DoF), and $H_{\mathrm{SOC}} = \xi \mathbf{L} \cdot \mathbf{S}$ captures spin-orbit coupling with coupling strength ξ. We will focus on a two-orbital two-spin model system, and our goal is to block diagonalize this Hamiltonian, decoupling spin DoF.

Written in the basis $\{|1\uparrow\rangle, |1\downarrow\rangle, |2\uparrow\rangle, |2\downarrow\rangle\}$, the most general H_0 is

$$\mathbf{H}_0 = \begin{pmatrix} E_1 & 0 & V & 0 \\ 0 & E_1 & 0 & V \\ V & 0 & E_2 & 0 \\ 0 & V & 0 & E_2 \end{pmatrix}, \tag{E1}$$

where E_1 and E_2 label orbital energies and V denotes coupling between the two orbitals. The spin-orbit coupling matrix $\mathbf{H}_{\mathrm{SOC}}$ can be constructed by calculating matrix elements $\langle\alpha m|H_{\mathrm{SOC}}|\beta n\rangle = \xi\frac{\hbar}{2}\mathbf{L}_{mn} \cdot \langle\alpha|\boldsymbol{\sigma}|\beta\rangle$ where m and n label orbital 1 and 2, and α and β represent spin up and down electrons. Since the spatial orbitals m and n can always be chosen to be real functions, $\mathbf{L}_{mn}$ is purely imaginary, and so $\mathbf{L}_{mm} = 0$. Therefore,

$$\mathbf{H}_{\mathrm{SOC}} = \xi\frac{\hbar}{2}\begin{pmatrix} 0 & 0 & L^z_{12} & L^x_{12} - iL^y_{12} \\ 0 & 0 & L^x_{12} + iL^y_{12} & -L^z_{12} \\ L^z_{21} & L^x_{21} - iL^y_{21} & 0 & 0 \\ L^x_{21} + iL^y_{21} & -L^z_{21} & 0 & 0 \end{pmatrix} \equiv \begin{pmatrix} \mathbf{0} & \mathbf{A} \\ \mathbf{A}^\dagger & \mathbf{0} \end{pmatrix},$$

where $\mathbf{A}$ is anti-Hermitian and can be diagonalized $\mathbf{A} = \mathbf{U}\mathbf{a}\mathbf{U}^\dagger$. Here $\mathbf{U}\mathbf{U}^\dagger = \mathbf{I}$ and

$$\mathbf{a} = \begin{pmatrix} a & 0 \\ 0 & -a \end{pmatrix},$$

where $a = i\xi\hbar|\mathbf{L}_{12}|/2$ is purely imaginary (and so $a^* = -a$). We can then transform $\mathbf{H}_{\mathrm{SOC}}$ to a new basis $\{|1\uparrow'\rangle, |1\downarrow'\rangle, |2\uparrow'\rangle, |2\downarrow'\rangle\}$ as follows:

$$\mathbf{H}_{\mathrm{SOC}} \rightarrow \mathbf{H}'_{\mathrm{SOC}} = \begin{pmatrix} \mathbf{U} & \mathbf{0} \\ \mathbf{0} & \mathbf{U} \end{pmatrix}\begin{pmatrix} \mathbf{0} & \mathbf{A} \\ \mathbf{A}^\dagger & \mathbf{0} \end{pmatrix}\begin{pmatrix} \mathbf{U}^\dagger & \mathbf{0} \\ \mathbf{0} & \mathbf{U}^\dagger \end{pmatrix} = \begin{pmatrix} \mathbf{0} & \mathbf{a} \\ \mathbf{a}^\dagger & \mathbf{0} \end{pmatrix}. \tag{E2}$$

Note that this transformation involves a rotation only for spin DoF. That is, $\mathbf{H}_0$ is invariant under this transformation. By reordering the new basis $\{|1\uparrow'\rangle, |1\downarrow'\rangle, |2\uparrow'\rangle, |2\downarrow'\rangle\}$ to $\{|1\uparrow'\rangle, |2\uparrow'\rangle, |1\downarrow'\rangle, |2\downarrow'\rangle\}$ in Eqs. (E1) and (E2), we recover Eq. (11).

---

[1] A. Fert, Rev. Mod. Phys. **80**, 1517 (2008).

[2] I. Žutić, J. Fabian, and S. Das Sarma, Rev. Mod. Phys. **76**, 323 (2004).

[3] D. Ralph and M. Stiles, J. Magn. Magn. Mater. **320**, 1190 (2008).

[4] S. Maekawa, H. Adachi, K.-I. Uchida, J. Ieda, and E. Saitoh, J. Phys. Soc. Jpn. **82**, 102002 (2013).

[5] S. Maekawa, S. O. Valenzuela, E. Saitoh, and T. Kimura, *Spin Current* (Oxford University Press, Oxford, 2017), Vol. 22.

[6] S. Sanvito, Chem. Soc. Rev. **40**, 3336 (2011).

[7] N. Nagaosa, J. Sinova, S. Onoda, A. H. MacDonald, and N. P. Ong, Rev. Mod. Phys. **82**, 1539 (2010).

[8] M. Z. Hasan and C. L. Kane, Rev. Mod. Phys. **82**, 3045 (2010).

[9] B. Göhler, V. Hamelbeck, T. Z. Markus, M. Kettner, G. F. Hanne, Z. Vager, R. Naaman, and H. Zacharias, Science **331**, 894 (2011).

[10] V. Kiran, S. R. Cohen, and R. Naaman, J. Chem. Phys. **146**, 092302 (2017).

[11] Y.-H. Kim, Y. Zhai, H. Lu, X. Pan, C. Xiao, E. A. Gaulding, S. P. Harvey, J. J. Berry, Z. V. Vardeny, J. M. Luther, and M. C. Beard, Science **371**, 1129 (2021).

[12] A. C. Aragonès, E. Medina, M. Ferrer-Huerta, N. Gimeno, M. Teixidó, J. L. Palma, N. Tao, J. M. Ugalde, E. Giralt, I. Díez-Pérez *et al.*, Small **13**, 1602519 (2017).

[13] R. Naaman, Y. Paltiel, and D. H. Waldeck, J. Phys. Chem. Lett. **11**, 3660 (2020).

[14] J. Gersten, K. Kaasbjerg, and A. Nitzan, J. Chem. Phys. **139**, 114111 (2013).

[15] A.-M. Guo and Q.-F. Sun, Phys. Rev. Lett. **108**, 218102 (2012).

[16] X. Yang, C. H. van der Wal, and B. J. van Wees, Phys. Rev. B **99**, 024418 (2019).

[17] S. Alwan and Y. Dubi, J. Am. Chem. Soc. **143**, 14235 (2021).

[18] V. V. Maslyuk, R. Gutierrez, A. Dianat, V. Mujica, and G. Cuniberti, J. Phys. Chem. Lett. **9**, 5453 (2018).

[19] M. S. Zöllner, S. Varela, E. Medina, V. Mujica, and C. Herrmann, J. Chem. Theory Comput. **16**, 2914 (2020).

[20] Y. Utsumi, O. Entin-Wohlman, and A. Aharony, Phys. Rev. B **102**, 035445 (2020).

[21] F. Evers, A. Aharony, N. Bar-Gill, O. Entin-Wohlman, P. Hedegård, O. Hod, P. Jelinek, G. Kamieniarz, M. Lemeshko, K. Michaeli, V. Mujica, R. Naaman, Y. Paltiel, S. Refaely-Abramson, O. Tal, J. Thijssen, M. Thoss, J. M. van Ruitenbeek, L. Venkataraman, D. H. Waldeck *et al.*, arXiv:2108.09998.

[22] F. D. Lewis, H. Zhu, P. Daublain, T. Fiebig, M. Raytchev, Q. Wang, and V. Shafirovich, J. Am. Chem. Soc. **128**, 791 (2006).

[23] D. N. Beratan, S. S. Skourtis, I. A. Balabin, A. Balaeff, S. Keinan, R. Venkatramani, and D. Xiao, Acc. Chem. Res. **42**, 1669 (2009).

[24] D. N. Beratan, Annu. Rev. Phys. Chem. **70**, 71 (2019).

[25] X. Bian, Y. Wu, H.-H. Teh, Z. Zhou, H.-T. Chen, and J. E. Subotnik, J. Chem. Phys. **154**, 110901 (2021).

[26] J. Fransson, Phys. Rev. B **102**, 235416 (2020).

[27] J. Fransson, J. Phys. Chem. Lett. **13**, 808 (2022).

[28] T. Culpitt, L. D. Peters, E. I. Tellgren, and T. Helgaker, J. Chem. Phys. **155**, 024104 (2021).

[29] M. Baer, *Beyond Born-Oppenheimer: Conical Intersections and Electronic Nonadiabatic Coupling Terms* (Wiley Online Library, 2006).

[30] H.-H. Teh, W. Dou, and J. E. Subotnik, Phys. Rev. B **104**, L201409 (2021).

[31] N. Bode, S. V. Kusminskiy, R. Egger, and F. von Oppen, Beilstein J. Nanotechnol. **3**, 144 (2012).

[32] B. B. Smith and J. T. Hynes, J. Chem. Phys. **99**, 6517 (1993).

[33] J.-T. Lü, M. Brandbyge, P. Hedegård, T. N. Todorov, and D. Dundas, Phys. Rev. B **85**, 245444 (2012).

[34] W. Dou, G. Miao, and J. E. Subotnik, Phys. Rev. Lett. **119**, 046001 (2017).

[35] F. Chen, K. Miwa, and M. Galperin, J. Phys. Chem. A **123**, 693 (2019).

[36] J.-T. Lü, M. Brandbyge, and P. Hedegård, Nano Lett. **10**, 1657 (2010).

[37] W. Dou and J. E. Subotnik, J. Chem. Phys. **148**, 230901 (2018).

[38] W. Dou and J. E. Subotnik, J. Chem. Phys. **146**, 092304 (2017).

[39] A. Nitzan, *Chemical Dynamics in Condensed Phases: Relaxation, Transfer and Reactions in Condensed Molecular Systems* (Oxford University Press, Oxford, 2006).

[40] J. P. Malhado and J. T. Hynes, J. Chem. Phys. **137**, 22A543 (2012).

[41] H. Haug and A.-P. Jauho, *Quantum Kinetics in Transport and Optics of Semiconductors* (Springer, Berlin, 2008), Vol. 2.

[42] W. Dou, C. Schinabeck, M. Thoss, and J. E. Subotnik, J. Chem. Phys. **148**, 102317 (2018).

[43] R. Naaman and D. H. Waldeck, J. Phys. Chem. Lett. **3**, 2178 (2012).

[44] R. Kapral, Annu. Rev. Phys. Chem. **57**, 129 (2006).

[45] W. Dou and J. E. Subotnik, Phys. Rev. B **97**, 064303 (2018).

[46] G. Stefanucci and R. Van Leeuwen, *Nonequilibrium Many-Body Theory of Quantum Systems: A Modern Introduction* (Cambridge University Press, Cambridge, 2013).

[47] S. Koseki, N. Matsunaga, T. Asada, M. W. Schmidt, and M. S. Gordon, J. Phys. Chem. A **123**, 2325 (2019).

[48] S. Varela, V. Mujica, and E. Medina, Phys. Rev. B **93**, 155436 (2016).